

# Impact of managed aquifer recharge structure on river flow regimes in arid and semi-arid climates

Navid Yaraghi<sup>a,\*</sup>, Anna-kaisa Ronkanen<sup>a</sup>, Hamid Darabi<sup>b</sup>, Bjørn Kløve<sup>a</sup>, Ali Torabi Haghighi<sup>a</sup>

<sup>a</sup> *Water, energy and environmental engineering research unit, University of Oulu, Oulu, Finland.*

<sup>b</sup> *Watershed management department, Sari Agriculture Science and Natural Resources University, Iran.*

---

## Abstract:

Managed aquifer recharge (MAR) structure is widely used to expand groundwater resources. In arid regions with flash flooding, MAR can also be used as a flood control structure to decrease peak discharge of rivers. In this paper, we present a method for quantifying the role of MAR in head water systems and assess its impact on the total water balance in a river basin. The method is based on rainfall-runoff modeling, reservoir flood routing, recharge analysis and river flow analysis. For the case selected, Kamal Abad MAR in Lake Maharlou basin in southern Iran, we analyzed changes in the downstream river regime using two scenarios (with MAR and without MAR) with different return periods. The results revealed a significant impact of MAR on river flow in terms of changes in flow timing, magnitude and variability. With MAR, the ephemeral river studied became disconnected from the main stream, albeit, whereas the case without MAR, floods with return period higher than 10 years would be connected to the downstream. Even though, MAR structures are useful in arid and semi-arid climates for irrigation water supply, their placing and designing need more attention. The developed method can be used to assess the impacts of MAR on river flow and find the best location for it to make the connection of the ephemeral river and downstream river, an issue which has not received much attention in hydrological research.

*Keywords:* Groundwater, Flood, Water retention, Dam, Irrigation

---

## 1. Introduction

In arid and semi-arid regions, groundwater (GW) provides a stable water resource and supply to meet agricultural demands (Prathapar et al., 2015). However, excessive GW exploitation due to expansion of agriculture has led to significant depletion of GW resources (Feike et al., 2017; Jyrkama and Sykes, 2007; Zaidi et al., 2015). This has effects on socioeconomic sectors and ecosystems onwards (UN-Water, 2016). Various artificial GW recharge techniques based on direct and indirect infiltration and percolation of surface water have been developed. One such method is Managed Aquifer Recharge (MAR) structure, which has been used to extend GW availability and restore GW levels after depletion (Ronayne et al., 2017). Especially in arid regions, MAR is an important method to maintain, enhance and secure stressed groundwater systems (Dillon, 2005; Dillon et al., 2019).

In Iran, a common MAR approach is to construct a dam above an aquifer to store water during flood events (Nafarzadegan et al., 2012). The set-up includes an earth embankment (a uniform earth dam), a free spillway to avoid flow over topping the embankment during extreme runoff conditions (e.g. high return period runoff) and an outlet pipe at the bottom of the structure (Ajmal et al., 2015; Sakakibara et al., 2017; Yiediboe et al., 2015). The benefit of the method depends on the amount of river water recharged to the aquifer and the reduction in peak flow achieved. Increased dams and artificial recharge can alter the downstream river regime (Ashraf et al., 2016; Askar, 2013; Torabi Haghighi and Kløve, 2015, 2013).

The main goal of this study is to develop a multi-stage framework for quantifying the impact of MAR on downstream river flow and to apply it in the case of the Kamal Abad MAR in Lake Maharlou

45 basin, southern Iran. In the method, flow regime change due to MAR are assessed along the river.  
46 Based on this the location of MAR structures can be optimized to lower the environmental impact  
47 and sustain sufficient flow in the river channel. Each step of this multi-stage framework exists already  
48 and is well documented (Askar, 2013; Beven, 2012; Choudhary and Chahar, 2007; Ghahreman and  
49 Abkhezr, 2004; Ghayoumian et al., 2007; Jahanshahi and Zare, 2016; Mancosu et al., 2015; Wösten  
50 et al., 2013). However, in our novel approach these steps are combined in order to assess the impact  
51 of small structures, particularly MAR, on river flow regime and the efficiency of the structures. The  
52 aims of this study was to combine previously used procedures and focus on the stage of the river after  
53 MAR structure. Based on this we studied the impacts of MAR on the length of the river before it  
54 gets disappeared as it is common situation in arid climatic region.

## 55 **2. Material and Methods**

### 56 **2.1. Study area**

57 Fars province in southern Iran (27°30'-31° 42'N; 50°30'-55°36' E) occupies an area of about 133,299  
58 km<sup>2</sup> and covers 8.1% of Iranian territory (Nafarzadegan et al., 2012). Mean annual precipitation in  
59 the region is approximately 335 mm, with estimated actual evaporation of 220 mm and recharge of  
60 65 mm (Tavanpour and Ghaemi, 2016). Daily precipitation data for the present study, recorded at  
61 Sarvestan, the closest meteorological station to the study area were obtained from Fars regional water  
62 authority.

63 Fars province is an important agricultural region in Iran, producing cereal, citrus fruits, dates, sugar  
64 beet and cotton. About 94% of water consumption is in the agriculture sector, which dramatically  
65 adds to the water crisis in the region. Moreover, low irrigation efficiency, which has been estimated  
66 to be near 30%, intensifies utilization of water resources in Fars.

67 Low efficiency is due to lack of fundamental irrigation facilities, poor skill and education of farmers  
68 and poor governance of water resources in Iran. For instance, the average depletion of the GW level  
69 on the Arsanjan, Khir, Estahban and Niriz plains is estimated to be 12, 8, 9 and 6 m during the past  
70 16, 11, 11 and 13 years, respectively (Hojati and Boustani, 2010).

71 More than 500 MAR systems have been built (or are planned) on river tributaries in Fars province to  
72 increase GW storage (Subgroup, 2004). One of these, Kamal Abad MAR (Figure 1), was used as the  
73 case in this study. It is located in Sarvestan County (28°50'24.42" N, 52°28'45.10"E) and has the  
74 capability for storing roughly 680,000 m<sup>3</sup>. It was constructed on an ephemeral river on one of the  
75 sub-basins of Lake Maharlou, also known as Daryache-ye-Namak (which means salt lake), a shallow  
76 lake with maximum 220 km<sup>2</sup> surface area located south-east of Shiraz city in central Fars province.  
77 The sub-basin is 31 km<sup>2</sup> which is mainly covered with gramineous vegetation and shrubs. The length  
78 of the river is 13 km. The Kamal Abad MAR system is 3.60 km upstream from the confluence of the  
79 ephemeral river with the main river. The main soil type is fluvial stream bed armored with rock and  
80 coarse gravel, with hydraulic conductivity of  $5.10^{-4}$  m.s<sup>-1</sup> based on the field measurements. The  
81 fluvial stream bed thickness varies from 50 to 200 m (Torabi Haghighi et al., 2007).

82 Technically, Kamal Abad MAR comprises an embankment or earth dam with a horizontal drain  
83 (filter) in the downstream toe to control recharge and piping in body of structure. The embankment  
84 is 10 m in height at its highest point has a 1200-m length of crest. The water discharges to downstream  
85 through an outlet pipe (diameter 40 cm) located at the bottom of the structure, at 0.70 m above the  
86 embankment bed. An anti-seep collar is installed around the pipe as erosion protection. The step  
87 spillway is positioned 7 m from the bed of the MAR, to prevent flow over topping the earth dam  
88 (Torabi Haghighi et al., 2007).

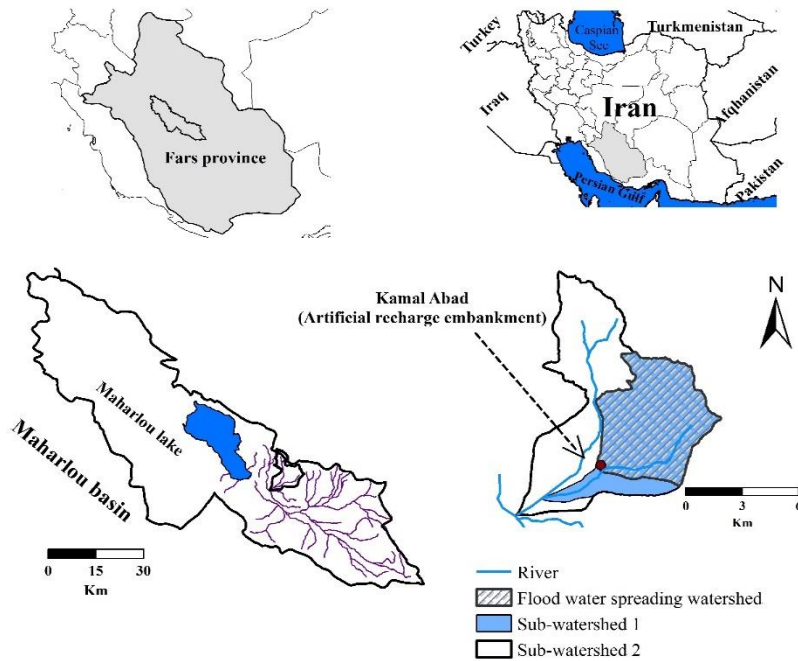


Figure 1: Maps showing the location of the study area in Lake Maharlou basin, Fars province, Iran, the Kamal Abad sub-basin and its managed aquifer recharge (MAR) embankment and the stream network.

101

102 The water volume for different elevations over the area affected by MAR was calculated using height  
 103 and area data Figure 2b obtained from a topographical map Figure 2a. The volume of the reservoir is  
 104  $260,000 \text{ m}^3$  and the area influenced is  $86,000 \text{ m}^2$  when the water level is 7 meters. The water volume  
 105 reaches  $680,000 \text{ m}^3$  is regard to maximum water level (10 m) in reservoir during designing flood  
 106 spillway.

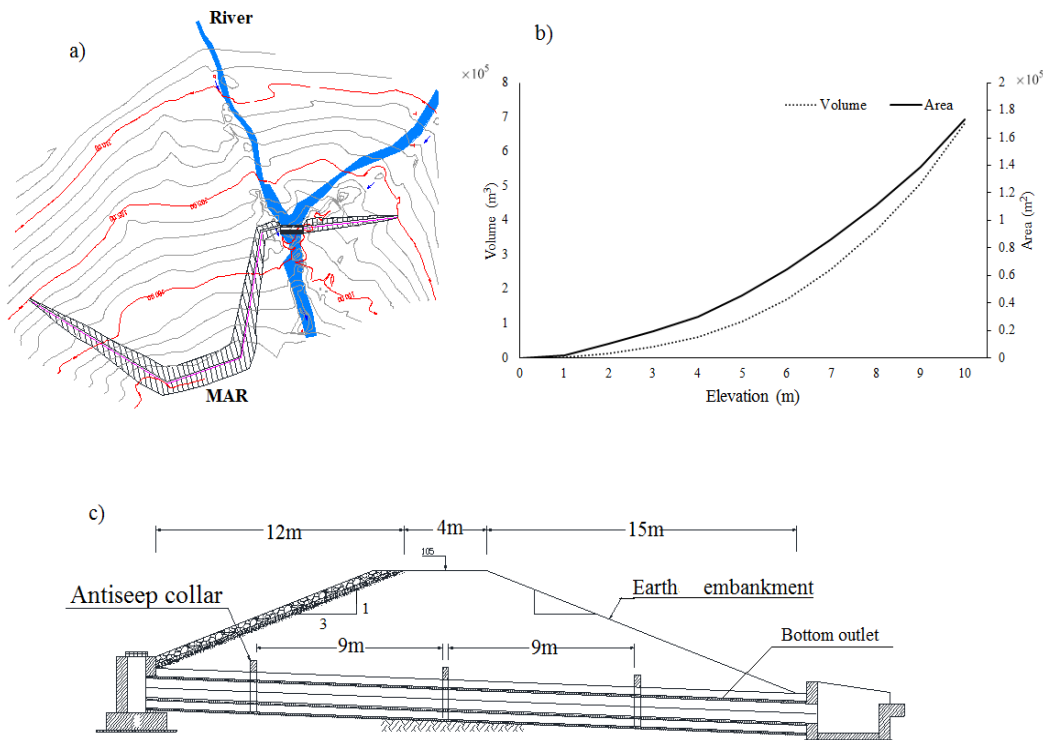


Figure 2: Technical information on Kamal Abad managed aquifer recharge (MAR) facility. a) Layout and topography, b) hypsometric curve of the reservoir (area-volume-elevation) and c) cross-section and bottom outlet.

## 2.2. Methodology

The framework we developed is based on rainfall-runoff modeling, reservoir and river flood routing and recharge analysis. First, the runoff to the Kamal Abad MAR system was estimated. This was considered to be the inflow to the river that Kamal Abad MAR has been constructed on. This was considered as inflow that is not altered by any structure as a first scenario called "without MAR". Then recharged and delay in the basin were calculated. The outflow from the MAR is called the second scenario (with MAR). Recharge occurs in the MAR basin and in the river upstream and downstream of the structure.

As the structure was constructed on an ephemeral river without any gauging station, maximum daily precipitation was used to assess rainfall return periods of 5, 10, 20, 50 and 100 years. Corresponding precipitation was estimated to be 21, 25, 32, 36 and 40 mm respectively. A rainfall intensity-duration-frequency (IDF) curve was developed (Figure 3a) based on the calculated maximum daily data using experimental Eq. 1 and 2 for the region derived by Ghahreman and Abkhezr (2004). They used long term rainfall data (1972-2004) to adopt the method to be valid also for estimating 10-year hourly rainfall.

$$P_{60}^{10} = 1.34 \times P_{24}^{0.694} \quad (1)$$

$$P_T^t = (0.4524 + 0.247 \ln(T - 0.6000))(0.3710 + 0.618t^{0.4484})P_{10}^{60} \quad (2)$$

where:  $P_{60}^{10}$  = one-hour precipitation with a 10-year return period (mm),

T = duration of precipitation (h)

t = return period (years)

$P_{24}$  = daily average precipitation (mm).

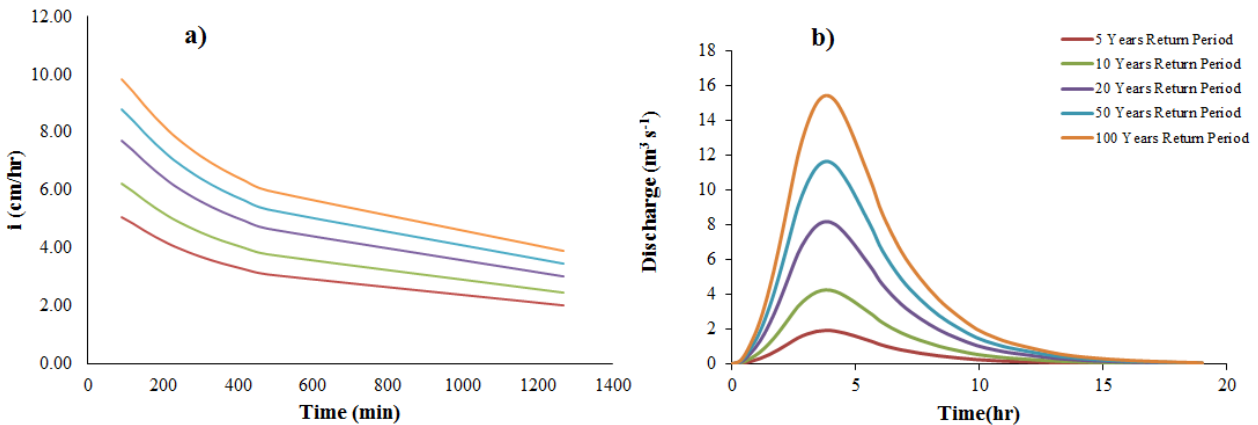


Figure 3: Rainfall and runoff for five different return periods in the study area: a) Rainfall intensity-duration-frequency and b) Hydrograph of the scenario "without MAR" derived by the USA Soil Conservation Service-Curve Number (SCS-CN) method.

In the absence of flow rate data for the study area, inflows were calculated using hydrographs with different return periods, by applying the synthetic unit hydrograph curve number (CN) method provided by the United States Soil Conservation Service (SCS) through rainfall-runoff modeling (Figure 3). In the SCS-CN method, curve number has a considerable influence on the inflow

147 hydrograph and needs to be selected carefully (Ajmal et al., 2015). The case study catchment  
 148 comprises poorly consolidated alluvial-pluvial deposits on young terraces consisting of sub-rounded  
 149 gravels and sand, silt and clay (Torabi Haghghi et al., 2007). Based on the exported information, the  
 150 soil was set in the group A, which means that it has low runoff potential, high infiltration rate and a  
 151 high rate of water transmission. For this group, the CN value is assumed to be 81. Another factor  
 152 which is essential in synthetic unit hydrograph curve number (CN) method is time of concentration.  
 153 Time of concentration is a conceptual value which is generally used to measure the basin's response  
 154 to the precipitation event. It can be known as a time that water needs to flow from the most remote  
 155 point in a basin to the outlet. Thus, it depends on the topography, geology and land use of the basin  
 156 (Chow et al., 1987). Time of concentration in our case study was 3.46 hours.

157 The outflow from the MAR structure (Figure 4) was calculated based on flood routing (Eq. 3-7) and  
 158 primary recharge (Eq. 8-9). Assessment of flood routing of the reservoir was based on the Level Pool  
 159 methodology defined by (Chow et al., 1987). The outlet diameter of the structure, the area-volume  
 160 curve (Figure 2b) and reservoir conditions were considered the main characteristics in flood routing.  
 161 Moreover, recharge water to the aquifer ( $q(t)$ ) was deducted from the outlet water amount to define  
 162 the total outflow from the structure, and thus bed soil material had a marked impact on the outflow.  
 163 Compared with the inflow, the outflow showed lower peak discharge and longer runoff duration  
 164 (Figure 4).

165

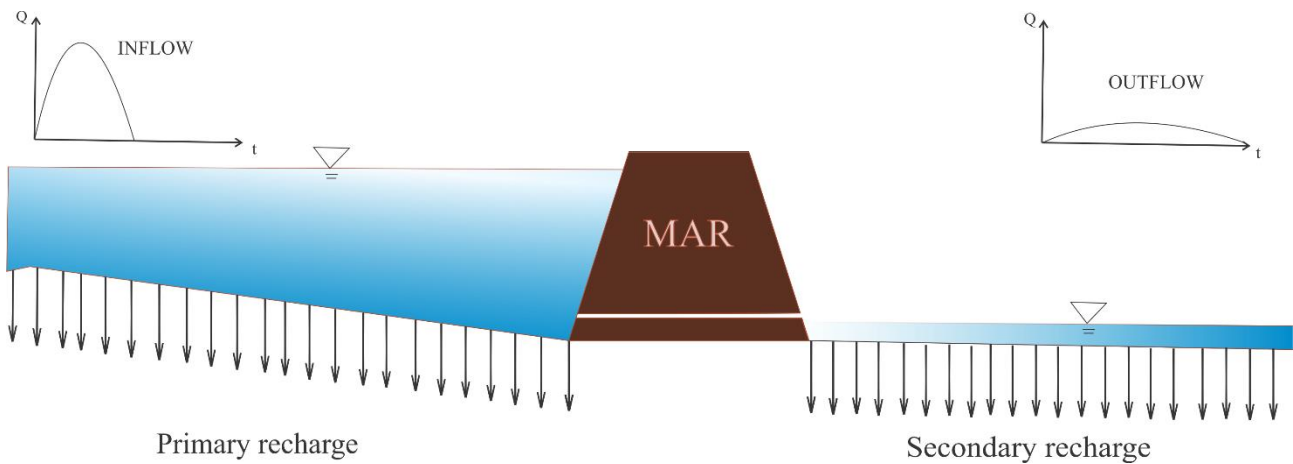


Figure 4: Schematic diagram showing the functioning of Kamal Abad Managed Aquifer recharge (MAR) structure.

166

$$Q = C * \left(\frac{\pi d^2}{4}\right) * (2 * g * h)^{0.5} \quad (3)$$

167

$$\frac{dS}{dt} = I(t) - Q(t) - q(t) \quad (4)$$

168

$$\int_{S_j}^{S_{j+1}} dS = \int_{j\Delta t}^{(j+1)\Delta t} I dt - \int_{j\Delta t}^{(j+1)\Delta t} Q dt - \int_{j\Delta t}^{(j+1)\Delta t} q dt \quad (5)$$

169

$$\frac{S_{j+1} - S_j}{\Delta t} = \frac{I_{j+1} + I_j}{2} - \frac{Q_{j+1} + Q_j}{2} - \frac{q_{j+1} + q_j}{2} \quad (6)$$

170

$$\frac{2S_{j+1}}{\Delta t} + Q_{j+1} + q_{j+1} = I_{j+1} + I_j + \frac{2S_j}{\Delta t} - Q_j - q_j \quad (7)$$

171

172

173 Where: C= Coefficient which is considered typically 0.6, d= Outlet diameter (m),

174  $q$ = recharge water to the aquifer ( $\text{m}^3\text{s}^{-1}$ )

175  $h$ = water elevation in reservoir (m),

176  $I$ = inflow ( $\text{m}^3\text{s}^{-1}$ ),

177  $Q$ = outflow ( $\text{m}^3\text{s}^{-1}$ ),

178  $S$ = storage ( $\text{m}^3$ ),

179  $t$ = time (s),

180  $j$ =interval factor.

181 Two type of flow changes were assumed to occur when MAR is applied, here defined as primary and  
182 secondary recharge. Primary recharge occurs through reservoir recharge from the pond of the MAR  
183 (which is considered the main recharge process). Secondary recharge occurs in the river downstream  
184 of the MAR structure Figure 4.

185 The GEO-Studio SEEP (2007) was used to model the primary recharge pathways and estimate the  
186 magnitude of recharge water, which was assumed to be a function of water level in the reservoir.  
187 SEEP/W is formulated on the basis that the flow of water through both saturated and unsaturated soil  
188 follows Darcy's Law which states that (GEO-SLOPE International Ltd., 2013):

$$189 \quad q = K * i \quad (8)$$

190 Where:

191  $q$  = specific discharge ( $\text{m s}^{-1}$ ),

192  $K$  = hydraulic conductivity ( $\text{m s}^{-1}$ ),

193  $i$  = gradient of total hydraulic head

194 Therefore, the general governing differential equation for two-dimensional steady state seepage can  
195 be expressed as:

$$196 \quad K_x \left( \frac{\partial^2 H}{\partial x^2} \right) + K_y \left( \frac{\partial^2 H}{\partial y^2} \right) + Q = 0 \quad (9)$$

197 Where:

198  $K_x$  = hydraulic conductivity in the x-direction ( $\text{m s}^{-1}$ )

199  $K_y$  = hydraulic conductivity in the y-direction ( $\text{m s}^{-1}$ )

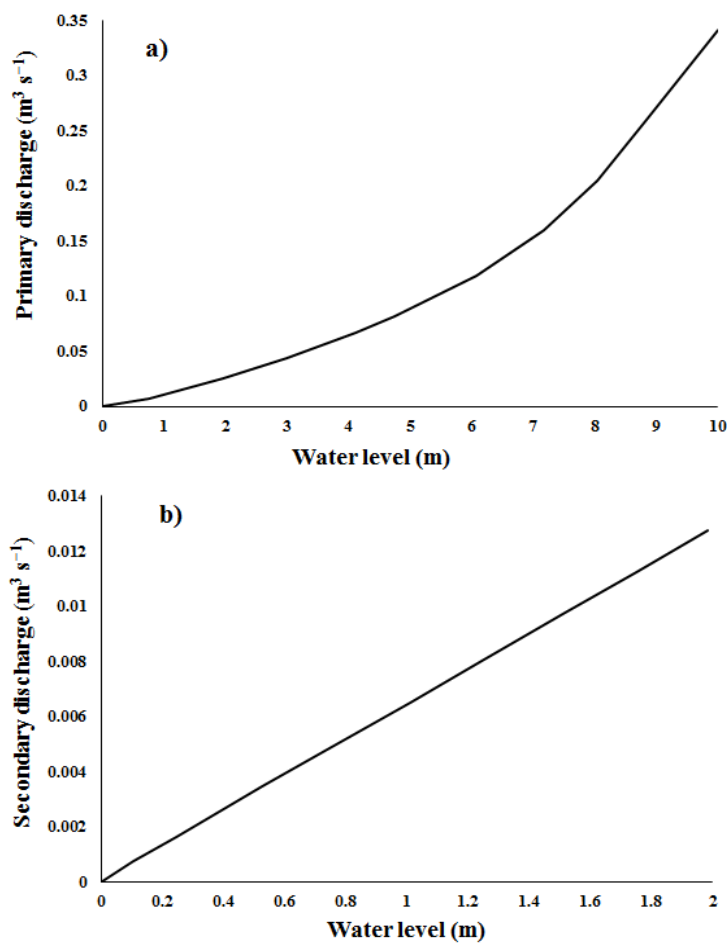
200  $H$  = total head (m)

201  $Q$  = applied boundary flux ( $\text{m s}^{-1}$ )

202 For the GEO-Studio SEEP model, the seepage through the dam was calculated by setting the  
203 boundary condition (BC) at water level in the pond and at atmospheric pressure outside the pond  
204 (after the MAR structure). The BC in the infiltration basin behind the MAR structure is a function of  
205 water level in the reservoir ( $H$ ), which varies between 0 and 10 m. It was assumed that the water  
206 entering the MAR earth dam also recharges the aquifer. Infiltration through the pond was calculated  
207 for a 1-m section and multiplied by the wet area to obtain the total water flux for different  $H$  (0-10m).  
208 By considering different upstream boundary conditions (different values of  $H$  in Eq. 9), the  
209 relationship between recharged flow and water elevation in the reservoir was estimated and

210 represented as the primary recharge rating curve (Figure 5a). Due to the shape of reservoir, the wet  
211 area increase with depth which effect the shape of the primary recharge rating curve (Figure 5 a).

212 The secondary recharge was also determined using the GEO-Studio/SEEP model (2007). Secondary  
213 recharge is a function of water level in river (can be varied spatially and temporally) and hydraulic  
214 conductivity of the river bed. Potential recharge face BC was selected for river edges (wetted  
215 perimeter), indicating that no additional stream water was added to or taken from the river. As the  
216 river flows only during large rainfall events, we assume no groundwater inflows to the river and the  
217 river is considered a “loosing river”. Also, the river has no inflows from tributaries after the MAR  
218 structure, so there is no need to consider inflows to the river system. The seepage through the river  
219 was estimated for different water levels in the river (0-2 m). Different values of seepage flow for 1 m  
220 length of the river was derived from the GEO-Studio/SEEP model and represented as recharge rating  
221 curve of the river (Figure 5 b). Due to a small increase of wet area by increasing water level, the curve  
222 obtained is linear.



237

Figure 5: Recharge rating curve for a) the Kamal Abad managed aquifer recharge (MAR) reservoir (primary recharge) and b) along the 1-m river length assumed for exfiltration (secondary recharge).

240

241

242

243

244 HEC-RAS (Version 5.0.3) was used to obtain the value of water level in the river for different  
 245 flowrates 0 to 20 m<sup>3</sup> s<sup>-1</sup> (Figure 6). Totally 10 cross sections of the river (mean width of 60 m and  
 246 the maximum water depth of 2 m) was set after the MAR structure for 3600 m river length. According  
 247 to field investigations (Torabi Haghghi et al., 2007) and classification of the river bed material, the  
 248 selected Manning number for the river is 0.038.

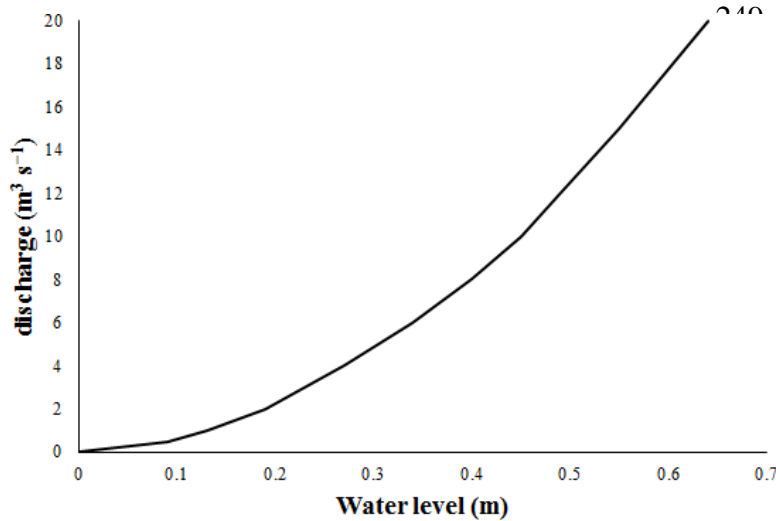


Figure 6: River rating curve (river discharge as a function of water table) derived using HEC-RAS River Analysis System.

257

258 To estimate the river flow alteration after the MAR structure and determine the length of the river  
 259 before the river flow disappeared, the following multi-stage framework was developed (Figure 7).

260

261

262

263

264

265

266

267

268

269

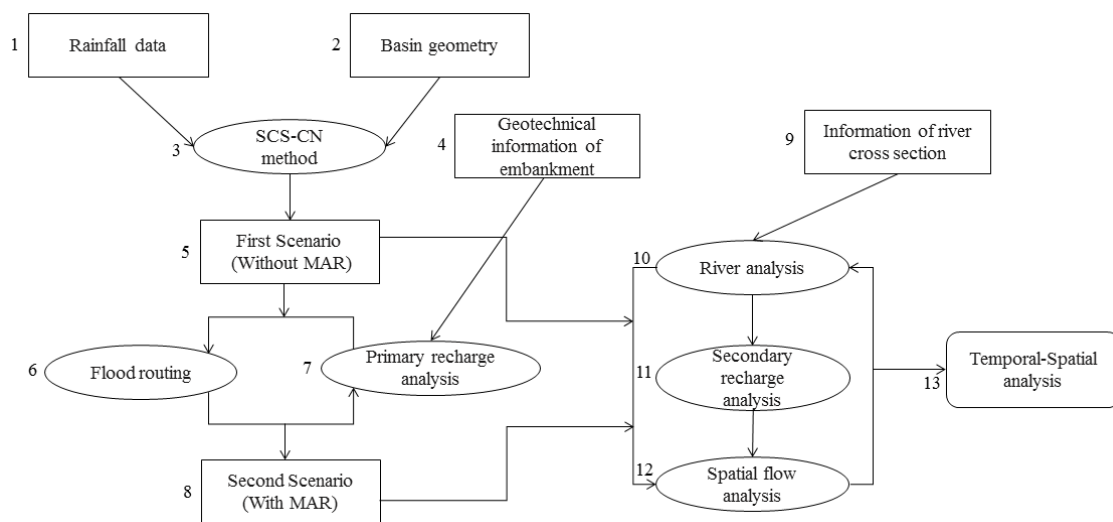


Figure 7: Multi-stage framework flow chart for managed aquifer recharge (MAR) applications.

270 There are several input in the framework. First hydrographs with different return periods (the inflow  
 271 in the river) is determined by SCS-CN method (item 3 in the Figure 7) where basin geometry and  
 272 rainfall data are needed to estimate the flow in the river in the scenario Without MAR (item 5). After  
 273 this, primary recharge magnitude is calculated as shown in Figure 6a. The river flow is also the input  
 274 for the flood routing (item 6) and primary recharge analysis (item 7) functions, which run  
 275 simultaneously to produce outflow from the MAR which is the scenario named with MAR (item 8).  
 276 Both scenarios are basic requirements for the further analysis (river Analysis, secondary recharge



277 analysis and spatial flow analysis) which are run simultaneously. The main part of the procedure,  
278 which clarifies the distance of river before the river water disappeared after the structure, is  
279 represented by these three modeling stages (items 10-12) and the result of the framework is obtained  
280 at item 13 which gives us the distance that river disappears at.

281 The distance between structure outlet and the point at which the river connect to the next stream is  
282 considered as the main river section influenced by MAR. The river is divided into 10-cm longitudinal  
283 elements to calculate the outflow from each element after secondary recharge application. The  
284 calculation starts at the first element, for which inflow is the outflow from the bottom outlet, and then  
285 the outflow of the first element is the inflow for the next one. Based on the magnitude of flow and  
286 rating curve of the river, the water level in the current element of the river can be estimated. Based  
287 on the water level in this element and rating curve of secondary recharge, the magnitude of recharge  
288 along the specific element is estimated. The recharge flow is subtracted from river flow serving as  
289 inflow for the next element. The interaction between the secondary recharge rating curve and river  
290 rating curve is the main key for solving our conceptual model.

291 The calculation of river flow is continued until the difference between inflow and outflow of each  
292 element reaches  $1.10^{-3} \text{ m}^3 \text{ s}^{-1}$ . The flow routing to the next element is continued until all flow seeps  
293 along the river (river disappears) or the river joins the downstream river. Through this multi-stage  
294 framework, the flow, water level and recharge flow at different points in different times can be  
295 specified. The calculation is carried out for both scenarios, to discover the response of the river system  
296 along the river. Comparisons between scenarios can reveal the impact of MAR on flow conditions in  
297 the downstream river. Technically, the framework is developed in MATLAB using input data derived  
298 from SCS-CN method and HEC-RAS & GEO-STUDIO/SEEP 2007 software.

299

### 3. Results

300

#### 3.1. Impact of MAR on river flow hydrographs

301

302

303

304

305

306

The Kamal Abad MAR changed the river hydrograph by lowering the peak discharge and markedly lengthening the base time (see Figure 8, transformed hydrographs in red and primary recharge hydrograph in black). The peak of inflow for 5, 10, 20, 50, and 100-year return period was calculated to be 1.92, 4.25, 8.16, 11.63 and 15.46  $\text{m}^3\text{s}^{-1}$ , but due to MAR they were reduced to 0.48, 0.59, 0.67, 0.70 and 0.72  $\text{m}^3\text{s}^{-1}$  respectively. Furthermore, the base time for outflow from the MAR increased considerably, for a flood with a 100-year return period from 20 to 130 hours.

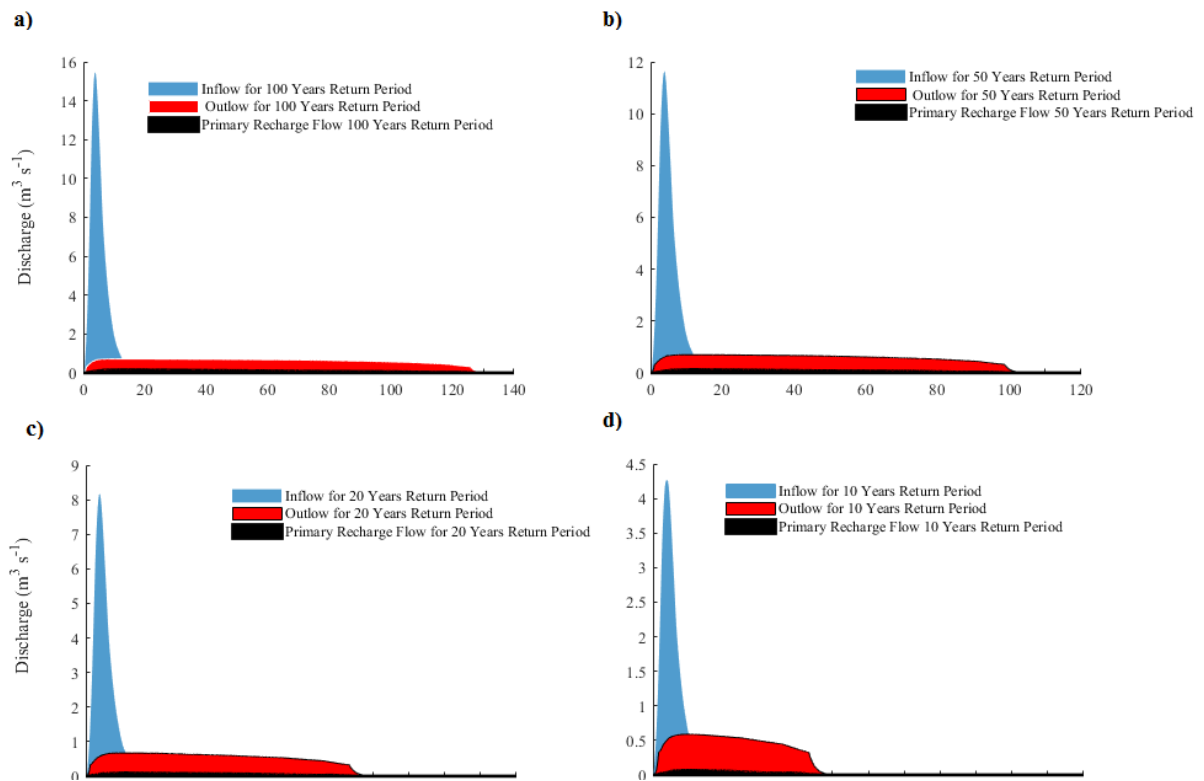


Figure 8: Inflow, outflow and primary recharge flow rate for Kamal Abad managed aquifer recharge during a) 100-year, b) 50-year, -c) 20-year and d) 10-year return periods.

307

308

#### 3.2. MAR and increased GW recharge

309

310

311

312

313

The MAR structure increased primary and secondary recharge in the river. The secondary recharge increased as the flow duration increased in the river section connected to the aquifer. The primary recharge volume to the aquifer at the central cross-section of the MAR during flood routing was 6644, 18977, 41964, 65972 and 95388  $\text{m}^3$  for a 5, 10, 20, 50 and 100 years return period, respectively (Figure 9).

314

315

316

317

318

The secondary recharge for “with MAR” scenario varied between 29,000 and 190,000  $\text{m}^3$  for different floods of 5 to 100 years return periods (Figure 9). The amount of secondary recharge was significantly more than primary recharge due to longer runoff duration and bigger area for seepage potential along the river, which allow more recharge (Figure 9). The MAR increase the recharge volume by about 18-33% in the aquifer.

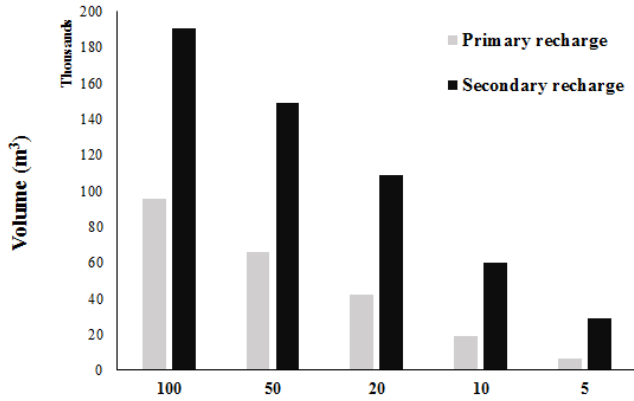


Figure 9: Comparison of primary and secondary recharge at Kamal Abad managed aquifer recharge for different return periods.

327

### 3.3. Spatial-temporal flow alteration in river flow

328

329

330

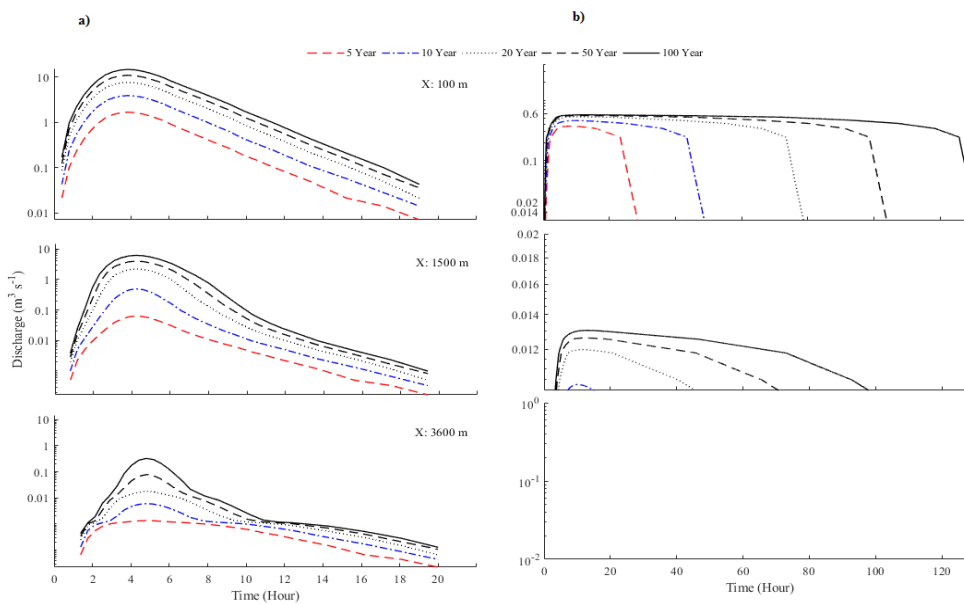
331

332

333

334

The hydrographs for both scenarios (With MAR and Without MAR) diminished along the river due to secondary recharge (Figure 10). The distance from the outlet of the MAR structure to the downstream river was approximately 3600 m. It was calculated that "without MAR" scenario with a 100, 50, 20, 10 and 5 years return period would last for 5753, 5214, 4604, 3796 and 3036 m of river length, which means that only floods with a 10 years return period or more can meet the downstream river as seen in Figures 10 and 11.



335

336

337

338

Figure 10: Spatial flow analysis along the river for the a) without MAR scenario and b) with MAR scenario for Kamal Abad MAR with different return periods (X=the distance from the MAR outlet).

339

340

341

342

343

At the downstream of MAR, the river disappeared at a maximum of 1500 m distance from the MAR structure. This represented a significant change, as before construction of Kamal Abad MAR floods with a 10 year return period or higher contributed to downstream discharge. In Figure 11, a decline in discharge of scenarios for different return periods along the river channel can be seen. Due to MAR, the flow with maximum peak discharge of  $0.2 \text{ m}^3 \text{ s}^{-1}$  occurs at 500 m distance from the outlet

344 pipe, whereas before construction of MAR this discharge happens after 4000 m. Without MAR  
 345 construction and the primary recharge to the aquifer, the flow could join to the downstream river. The  
 346 results show if the MAR was constructed in 1 km further downstream, water reaches the river  
 347 downstream even with primary recharge (Figure 11).

348

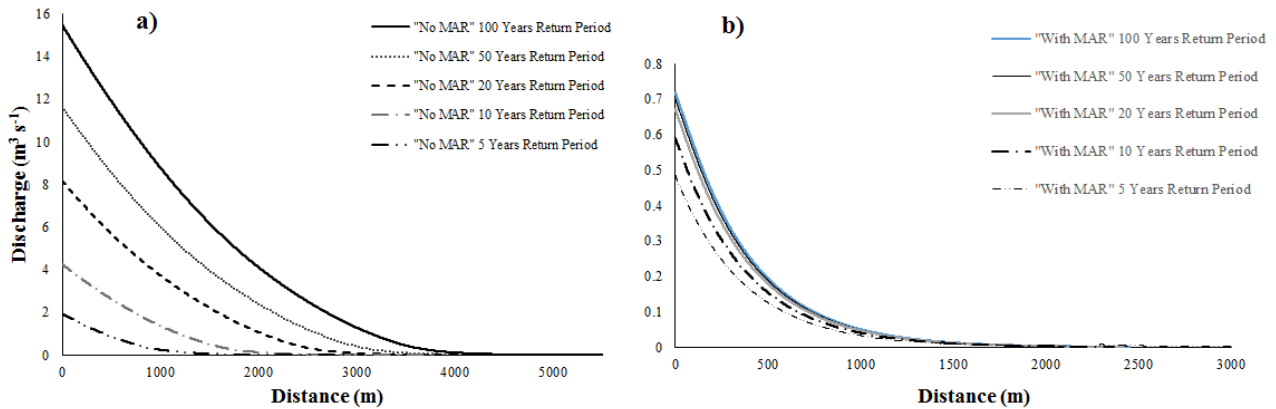


Figure 11: Decline in maximum discharge with increasing distance from the Kamal Abad MAR for two scenarios a) "w~~o~~without MAR b) w~~o~~with MAR.

349

350

#### 351 4. Discussion

352 A benefit of MAR structures is to increase recharge to allow for stable and increased groundwater  
 353 supply (Dillon, 2005). This has allowed agriculture to develop in semiarid regions providing many  
 354 socio-economic benefits. However, the impacts of MAR at catchment scale or on river flows has not  
 355 been much studied.

356 Increased irrigation in arid regions, such as Iran, has significantly reduced river flow to  
 357 downstream water systems (Fazel et al., 2017). This means that ephemeral rivers such as the study  
 358 case dry up more often. To solve this, even more MAR structures have been constructed in the Lake  
 359 Maharlou watershed, which can be predict to accelerate the observed decline in water levels in the  
 360 region. Based on the results of this study, the existing MAR structure seems to be over-designed, as  
 361 the storage capacity of Kamal Abad MAR is about 680,000  $\text{m}^3$ , while the volume of the flood with  
 362 a 100-year return period is only about 285,000  $\text{m}^3$ . The framework presented here is the first  
 363 systematic approach to study the impacts of MAR on river regimes. However, there are some  
 364 uncertainties, for example lack of information on (i) field conditions, (ii) the rainfall-runoff modeling  
 365 component, (iii) soil properties, (iv) recharge and (v) river analysis components.

366 Hydraulic conductivity and river morphology would most certainly have an influence on primary  
 367 (before MAR) and secondary (After MAR) recharge. Generally the hydraulic conductivity of the soil  
 368 is seen the most important characteristic to control recharge (Wösten et al., 2013). Also in our  
 369 framework, recharge analysis, particularly from the river bed, plays a major role in revealing the  
 370 effects of MAR on river flow. To model recharge flow in this study, hydraulic conductivity of soil  
 371 was based on a few field samples taken from the reservoir and the river bed materials (Torabi  
 372 Haghghi et al., 2007). Despite of the lack of the data, the determined soil hydraulic conductivity  
 373 values used agrees with the range of soil properties in the available standard. For instance, under  
 374 Swiss Standard SN 670 010b, which has been used in previous studies (Gashti et al., 2014; Yiediboe  
 375 et al., 2015), the river bed soil has been classified to be well graded gravel and sandy gravel with little

376 or no fines (similar to observed conditions in Kamal Abad) and the hydraulic conductivity of the soil  
377 could vary between 0.0005 and 0.05 m s<sup>-1</sup>. For Kamal Abad, we considered value of 0.00075 ms<sup>-1</sup>  
378 for river bed and embankment.

379 Although the river water level fluctuated in both the primary and secondary recharge analysis, to  
380 simplify the process in the framework the recharge rating curve was developed under a quasi-steady-  
381 state conditions by simulation of recharge for variable water levels. This simplification is justified to  
382 analyze the overall effects of MAR would not have a large effect on the recharge or flow. A full  
383 transient simulation would require more time and resources and this steady-state assumption is the  
384 first step for understanding the MAR impacts on the flow regime of the river. Also sedimentation  
385 effect on seepage flows and evaporation losses in the reservoir was not considered which is counted  
386 as future.

387

## 388 **5. Conclusion**

389 Managed Aquifer Recharge (MAR) is a promising method to increase groundwater recharge and  
390 reduce floods in arid and semi-arid regions. However, MAR has the potential to change river flows  
391 significantly, an issue that has not been studied sufficiently in the past. In this study, we developed a  
392 framework for quantifying the impact of MAR on river flows, based on different flood return periods.  
393 The results showed that MAR increased primary recharge 18–33% as it has been supposed to do but  
394 also increase the secondary recharge from the downstream river to the GW. Increasing secondary  
395 recharge reduces the flow in the ephemeral river which reduces its connection to the main tributary,  
396 which might be important to consider in some cases. As MAR influences river flow, careful planning  
397 is required when using MAR as a method to restore GW systems and increase crop irrigation.

398

## 399 **References**

- 400 Ajmal, M., Moon, G. woo, Ahn, J. hyun, Kim, T. woong, 2015. Investigation of SCS-CN and its  
401 inspired modified models for runoff estimation in South Korean watersheds. *Journal of Hydro-*  
402 *Environment Research* 9, 592–603. doi:10.1016/j.jher.2014.11.003
- 403 Ashraf, F. Bin, Torabi Haghghi, A., Marttila, H., Kløve, B., 2016. Assessing impacts of climate  
404 change and river regulation on flow regimes in cold climate : A study of a pristine and a regulated  
405 river in the sub-arctic setting of Northern Europe. *Journal of Hydrology* 542, 410–422.  
406 doi:10.1016/j.jhydrol.2016.09.016
- 407 Askar, M.K., 2013. Rainfall-runoff model using the SCS-CN method and geographic information  
408 systems: A case study of Gomal River watershed. *WIT Transactions on Ecology and the*  
409 *Environment* 178, 159–170. doi:10.2495/WS130141
- 410 Beven, K.J., 2012. Rainfall-runoff modelling: the primer, *Rainfall-Runoff Modelling: The Primer:*  
411 *Second Edition*. doi:10.1002/9781119951001
- 412 Choudhary, M., Chahar, B.R., 2007. Recharge/seepage from an array of rectangular channels. *Journal*  
413 *of Hydrology* 343, 71–79. doi:10.1016/j.jhydrol.2007.06.009
- 414 Chow, V. Te, Maidment, D.R., Mays, L.W., 1987. *Applied Hydrology*.
- 415 Dillon, P., 2005. Future management of aquifer recharge 313–316. doi:10.1007/s10040-004-0413-6
- 416 Dillon, P., Stuyfzand, P., Grischek, T., Lluria, M., Pyne, R.D.G., Jain, R.C., Bear, J., Schwarz, J.,  
417 Wang, W., 2019. Sixty years of global progress in managed aquifer recharge 1–30.

- 418 Fazel, N., Torabi Haghighi, A., Kløve, B., 2017. Analysis of land use and climate change impacts by  
419 comparing river flow records for headwaters and lowland reaches. *Global and Planetary Change*  
420 158, 47–56. doi:10.1016/j.gloplacha.2017.09.014
- 421 Feike, T., Khor, L.Y., Mamitimin, Y., Ha, N., Li, L., Abdusalih, N., Xiao, H., Doluschitz, R., 2017.  
422 Determination of cotton farmers' irrigation water management in arid Northwestern China.  
423 *Agriculture Water Management* 187, 1–10.
- 424 Gashti, E.H.N., Malaska, M., Kujala, K., 2014. Structural Behaviour of Concrete Energy Piles in  
425 Thermal Loadings 8, 1248–1252.
- 426 GEO-SLOPE International Ltd., 2013. Seepage Modeling with SEEP/W 197.
- 427 Ghahreman, B., Abkhezr, H., 2004. Improve the Intensity-Duration-Frequency equations in Iran.  
428 *Science and Technology of Agriculture and Natural Resources*.
- 429 Ghayoumian, J., Mohseni Saravi, M., Feiznia, S., Nouri, B., Malekian, A., 2007. Application of GIS  
430 techniques to determine areas most suitable for artificial groundwater recharge in a coastal  
431 aquifer in southern Iran. *Journal of Asian Earth Sciences* 30, 364–374.  
432 doi:10.1016/j.jseaes.2006.11.002
- 433 Hojati, M.H., Boustani, F., 2010. An Assessment of groundwater crisis in Iran Case study: Fars  
434 province. *World academy of science, Engineering and Technology* 4, 10–26.
- 435 Jahanshahi, R., Zare, M., 2016. Journal of African Earth Sciences Hydrochemical investigations for  
436 delineating salt-water intrusion into the coastal aquifer of Maharlou Lake, Iran. *Journal of*  
437 *African Earth Sciences* 121, 16–29. doi:10.1016/j.jafrearsci.2016.05.014
- 438 Jyrkama, M.I., Sykes, J.F., 2007. The impact of climate change on spatially varying groundwater  
439 recharge in the grand river watershed (Ontario). *Journal of Hydrology* 338, 237–250.  
440 doi:10.1016/j.jhydrol.2007.02.036
- 441 Mancosu, N., Snyder, R., Kyriakakis, G., Spano, D., 2015. Water Scarcity and Future Challenges for  
442 Food Production. *Water* 7, 975–992. doi:10.3390/w7030975
- 443 Nafarzadegan, A.R., Rezaeian Zadeh, M., Kherad, M., Ahani, H., Gharekhani, A., Karampoor,  
444 M.A., Kousari, M.R., 2012. Drought area monitoring during the past three decades in Fars  
445 province, Iran. *Quaternary International* 250, 27–36.
- 446 Prathapar, S., Dhar, S., Rao, G.T., Maheshwari, B., 2015. Performance and impacts of managed  
447 aquifer recharge interventions for agricultural water security: A framework for evaluation.  
448 *Agriculture Water Management* 159, 165–175.
- 449 Ronayne, M.J., Roudebush, J.A., Stednick, J.D., 2017. Analysis of managed aquifer recharge for  
450 retiming streamflow in an alluvial river. *Journal of Hydrology* 544, 373–382.  
451 doi:10.1016/j.jhydrol.2016.11.054
- 452 Sakakibara, K., Tsujimura, M., Song, X., Zhang, J., 2017. Spatiotemporal variation of the surface  
453 water effect on the groundwater recharge in a low-precipitation region: Application of the multi-  
454 tracer approach to the Taihang Mountains, North China. *Journal of Hydrology* 545, 132–144.  
455 doi:10.1016/j.jhydrol.2016.12.030
- 456 Subgroup, S., 2004. Proposal for artificial recharge projects in order to flood control to improve the  
457 quality and quantity of groundwater resources and reducing water crisis.
- 458 Tavanpour, N., Ghaemi, A.A., 2016. ZONING OF FARS PROVINCE IN TERMS OF RAIN-FED  
459 WINTER WHEAT CULTIVATION BASED ON PRECIPITATION AND ... trends in life

460 sciences.

461 Torabi Haghghi, A., Habibi, H., Dianatpour, A., Mprtazavi, R., 2007. Feasibility report of  
462 KamalAbad Artificial GroundWater Recharge Structure.

463 Torabi Haghghi, A., Kløve, B., 2015. *Limnologica* A sensitivity analysis of lake water level response  
464 to changes in climate and river regimes. *Limnologica* 51, 118–130.  
465 doi:10.1016/j.limno.2015.02.001

466 Torabi Haghghi, A., Kløve, B., 2013. Development of a general river regime index ( RRI ) for intra-  
467 annual flow variation based on the unit river concept and flow variation end-points. *Journal of*  
468 *Hydrology* 503, 169–177. doi:10.1016/j.jhydrol.2013.08.041

469 UN-Water, 2016. Water and jobs. United Nations World Water Assesement Programme,  
470 UNESCO, Paris, France.

471 Wösten, J.H.M., Verzandvoort, S.J.E., Leenaars, J.G.B., Hoogland, T., Wesseling, J.G., 2013. Soil  
472 hydraulic information for river basin studies in semi-arid regions. *Geoderma* 195–196, 79–86.  
473 doi:10.1016/j.geoderma.2012.11.021

474 Yiediboe, B., Lin, H.E., Jian, Y., Cong, L., Zhenliang, W., 2015. The Relationship between the  
475 Physical Properties of Soil and Shape Factors of its Fragmented Aggregates: A Two-  
476 Dimensional Digital Image Processing and Analysis Approach 3, 1–15.

477 Zaidi, F.K., Nazzal, Y., Ahmed, I., Naeem, M., Jafri, M.K., 2015. Identification of potential artificial  
478 groundwater recharge zones in Northwestern Saudi Arabia using GIS and Boolean logic. *Journal*  
479 *of African Earth Sciences* 111, 156–169. doi:10.1016/j.jafrearsci.2015.07.008

480

481

482

483

484